J Solid State Electrochem (2010) 14:1841–1846
DOI 10.1007/s10008-010-1016-x

ORIGINAL PAPER

Growth of V_2O_5 nanorods from ball-milled powders and their performance in cathodes and anodes of lithium-ion batteries

Alexey M. Glushenkov · Mohd Faiz Hassan · Vladimir I. Stukachev · Zaiping Guo · Hua Kun Liu · Gennady G. Kuvshinov · Ying Chen

Received: 20 November 2009 / Revised: 23 January 2010 / Accepted: 27 January 2010 / Published online: 23 February 2010
© Springer-Verlag 2010

Abstract The two-stage procedure of ball milling and annealing in air represents a prospective method of preparing nanorods of V_2O_5 with electrochemical properties suitable for the application in lithium-ion batteries. Commercially purchased V_2O_5 powder is milled in a ball mill as the first step of the synthesis. The as-milled precursor is subsequently annealed in air to produce the morphology of nanorods via solid-state recrystallization. We have recently investigated intermediate stages of the formation of nanorods, and this paper summarizes the synthesis method including the description of the current understanding of the growth mechanism. The obtained V_2O_5 nanorods have been assessed as an electrode material for both anodes and cathodes of lithium-ion batteries. When used in cathodes, the nanorods demonstrate a better retention of capacity upon cycling than that of the commercially available powder of V_2O_5. When used in anodes, the performances of nanorods and the reference V_2O_5 powder are similar to a large extent, which is related to a different operating mechanism of V_2O_5 in anodes. The experimentally observed capacity of V_2O_5 nanorods in an anode has stabilized at the level of about 450 mAh/g after few cycles.

Keywords Anodes · Ball milling powder · Cathodes · Lithium-ion batteries · Nanorods · Vanadium pentoxide

A. M. Glushenkov (✉) · Y. Chen
Institute for Technology Research and Innovation,
Deakin University,
Waurn Ponds, VIC 3217, Australia
e-mail: alexey.glushenkov@deakin.edu.au

M. F. Hassan · Z. Guo · H. K. Liu
Institute for Superconducting and Electronic Materials,
University of Wollongong,
Wollongong, NSW 2522, Australia

M. F. Hassan
Department of Science Physics,
University of Malaysia Terengganu,
Kuala Terengganu 20522, Malaysia

V. I. Stukachev · G. G. Kuvshinov
Department of Chemical Engineering,
Novosibirsk State Technical University,
Pr. Karla Marksa 20,
Novosibirsk 630092, Russia

Introduction

Vanadium pentoxide (V_2O_5) is a well-known candidate for cathodes in Li-ion batteries and electrochromic devices. However, the performance of conventional V_2O_5 powders in cathodes was significantly limited by a slow rate of lithium diffusion in the lattice and a low electronic conductivity. Recent research shows that the electrochemical performance of V_2O_5 can be improved by using nanostructured V_2O_5. Nanostructures of vanadium pentoxide were able to solve the conventional problems of low conductivity and slow lithium diffusion and provide an improved electrode performance in cathodes [1, 2]. V_2O_5 exhibits a high theoretical capacity of about 400 mAh/g [3] and can be an attractive candidate for cathodes.

V_2O_5 can also be used as an anode material with a high capacity in lithium-ion batteries. Although the possible capacity is quite attractive, there is virtually no literature on the subject. Liu et al. [4] have analyzed the anode performance of double-shelled V_2O_5-based nanocapsules.

Apart from V_2O_5, the nanocapsules contained 10 wt% of SnO_2. The material had a very high discharge capacity of 1,776 mAh/g in the first cycle, which dropped to about 1,000 mAh/g in the second discharge. After 50 cycles, the V_2O_5-based nanocomposite could deliver a reversible capacity of 673 mAh/g [4].

We have recently reported a novel preparation method for nanorods of V_2O_5 [5] where the nanorods with rectangular cross sections were formed via heating of ball-milled V_2O_5 powders in the atmosphere of air or O_2. The structural characterization demonstrated that the nanorods were elongated along the [010] direction and had the suppressed thickness along the [001] direction [5]. It has been noted [5] that these nanorods have a beneficial cycling stability when they are used as a cathode in a lithium battery.

Additional characterization of the material at the intermediate stages of growth has been conducted [6]. Here, we review our current understanding of the growth mechanism in the light of available data. The direct comparison of the electrochemical performance of V_2O_5 nanorods with that of the commercially available V_2O_5 powder (Sigma Aldrich) in both cathodes and anodes of lithium-ion batteries is presented in the second part of the paper.

Experimental

A steel magneto-ball mill was used for ball milling. Three grams of V_2O_5 powder (99.6% purity, Sigma Aldrich) were milled in argon atmosphere for 100 h at room temperature. The milled material was annealed at about 600 °C in air in two ways: (1) as a static layer on top of a substrate; (2) in a fluidized (vibrating) bed.

In order to perform static annealing, a thin layer of milled material was deposited onto the surface of a steel or oxidized silicon substrate. The layer density was typically about 3 mg/cm^2. The substrates covered with milled V_2O_5 powder were isothermally heated at 630 °C for various periods of time (between 1 min and 2 h). The substrates coated with V_2O_5 were inserted into the preheated furnace and pulled out quickly after the desired annealing time.

The fluidized bed conditions were achieved by vibrating a cylindrical quartz reactor with the diameter of 40 mm and the height of 200 mm. Milled V_2O_5 powder (1 g) was placed into the reactor, and the reactor was inserted into the furnace preheated to 600 °C.

The materials at various stages of growth were characterized by scanning electron microscopy (SEM), transmission electron microscopy (TEM), X-ray diffraction (XRD), low-temperature N_2 adsorption, and electron spin resonance (ESR). The data critical for basic understanding of the growth phenomenon are shown in the manuscript, and the rest of "raw" data can be found in [5, 6] if needed.

The nanorods obtained in a static layer at 630 °C in air after 5 min of annealing were used to assemble working electrodes. Approximately 250 mg of V_2O_5 nanorods have been prepared on steel substrates. The as-grown nanorods are attached to the substrates weakly. They have been removed from the substrates via simple scrapping using a scalpel. The obtained powder of nanorods was used for the assembly of electrodes via mixing with a binder and acetylene black and transferring the resulting slurry onto current collectors.

The cathode electrode was prepared as a thick film by a doctor-blade deposition of a slurry composed of 80 wt% V_2O_5 (active material), 10 wt% acetylene black (AB) (conductive additive), and 10 wt% polyvinylidene fluoride (PVDF) in *N*-methyl-2-pyrrolidinone onto an aluminum substrate (1 cm^2). After drying the electrode at 100 °C for 12 h under vacuum, it was compressed and then weighed. The electrochemical behavior of the materials was examined using CR2025 coin-type cells with lithium metal as the counter electrode, Celgard 25400 membrane as the separator, and 1 M $LiPF_6$ in a mixture of ethylene carbonate (EC) and dimethyl carbonate (DMC) (1:1 by volume) as the electrolyte. The cells were assembled in an argon-filled glove box (Mbraun, Unilab, Germany). The charge–discharge measurements were conducted at room temperature on a multi-channel battery cycler in the voltage range between 1.5–3.5 V vs. Li/Li^+ at a current density of 10 mA/g.

The anode electrode was prepared by a similar method. The weight ratio of the components of the slurry was 75 wt% V_2O_5, 20 wt% AB, and 5 wt% PVDF. The slurry was deposited onto a copper substrate (1 cm^2) to form the electrode. The electrolyte was 1 M $LiPF_6$ in a mixture of EC and DMC (1:1 by volume) and Celgard 2500 membrane was used as a separator. The cell was charged and discharged at the current rate of 30 mA/g over a voltage range of 0.01–3.0 V vs. Li/Li^+.

Results and discussion

Synthesis method

The annealing of the ball-milled material leads to the apparent changes in the morphology. The typical appearance of V_2O_5 after ball milling and 5 min of subsequent annealing at 630 °C is depicted in Fig. 1. The as-milled material (Fig. 1a) consists of rather irregular particles with a range of sizes. Annealing in air for 5 min leads to a very obvious change of morphology, and the material converts into a collection of elongated particles (Fig. 1b). XRD and electron diffraction tests confirm that the nanorods belong to the orthorhombic V_2O_5 phase (PDF file #41-1426). The structural characterization demonstrates that the nanorods are elongated along the [010] direction and have a

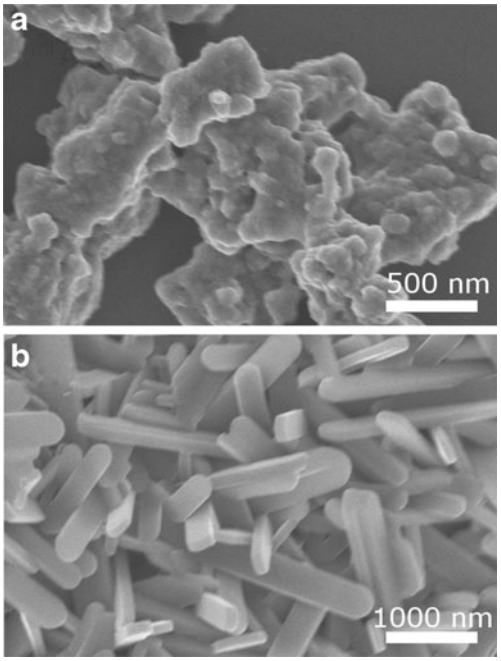

Fig. 1 SEM images of ball-milled powder before (**a**) and after annealing in air at 630 °C for 5 min (**b**)

suppressed thickness along the [001] direction. An interested reader can find the original XRD pattern of V_2O_5 nanorods and TEM data in our first report on the topic [5].

Additional characterization of the ball-milled materials and intermediate stages of growth (1 and 2.5 min) helped to provide insight into the formation mechanism of nanorods [6]. The studies of the ball-milled powder by XRD, TEM, and EPR methods (see [6] for original experimental data) indicated that the precursor after ball milling consisted of polycrystalline particles with typical grain (crystallite) sizes of 7–35 nm and random orientation of crystallites. More specifically, the particles in the milled powder should be understood not as individual polycrystalline particles but as porous aggregates of attached polycrystalline nanoparticles. The vanadium oxide was also reduced to some extent after ball milling, which was evident from the changes in lattice distances and the appearance of a signal at around 3400 Gauss in an EPR spectrum [6]. The stoichiometric V_2O_5 is EPR-silent, and the resonance signal in its ESR spectrum should be attributed to the appearance of paramagnetic V^{4+} species [7].

According to SEM and TEM results of the intermediate stages of growth (1 and 2.5 min) presented in [6], the agglomerates of initial polycrystalline particles convert into porous aggregates of single-crystalline nanoparticles. The individual nanoparticles are enlarged in a non-uniform fashion. Simultaneously, the reduced material gets gradually oxidized, and the missing oxygen atoms get incorporated into the material [6]. After the material reaches its stoichiometric composition, the [010] direction is becoming the direction of the quick growth. According to our observations [5], the surface diffusion plays an important part in the growth of nanorods at this stage, and the nanorods enlarge via coalescence (merging of the adjacent nanorods and reshaping). The resulting morphology is believed to satisfy the requirements of surface energy minimization, since {001} facets are the lowest energy surfaces in V_2O_5.

The inherent problem of the synthesis procedure is that the ball-milled vanadium oxide should be annealed as a thin film on the surface of a substrate. If the bulk amount of milled vanadium oxide is heated in a static bed, it tends to aggregate into a large brick due to the sintering. Meanwhile, the material in a free powder form is desired for many applications such as lithium-ion batteries, for example. We have demonstrated that annealing in a mobile bed can effectively minimize the issue of sintering and produce a larger amount of the nanorod powder. In two demonstration experiments, 1 g of the ball-milled powder was annealed in a fluidized (vibrating) bed at 600 °C for 5 and 60 min, respectively. In each experiment, the synthesis was conducted inside a quartz reactor which was vibrated vertically.

Figure 2 shows a photograph of 1 g of V_2O_5 nanorods produced after annealing in a fluidized (vibrating) bed for 5 min. The product of annealing is in a powder form. We have also demonstrated that the material remains in the powder form even after extended annealing for 60 min [5]. The SEM studies confirmed that nanorods are the dominating morphology in the powder. The results indicate that the use of a mobile bed for annealing of the precursor may lead to the production of this material in larger quantities. Although it is clear that some degree of agglomeration is unavoidable during the synthesis, the sintering of particles and formation of large bricks is significantly suppressed in comparison with the product of annealing in a static bed.

Fig. 2 One gram of V_2O_5 nanorod powder obtained after 5 min of annealing in a fluidized (vibrating) bed at 600 °C

The scheme of recrystallization of nanocrystalline V_2O_5 produced by ball milling at around 600 °C is summarized in Fig. 3. At the initial stage of recrystallization, the aggregates of polycrystalline nanoparticles tend to remove numerous grain boundaries and transform into aggregates of single-crystalline particles with a larger size and a limited area of contact between them. The oxidation of the initially reduced materials into stoichiometric V_2O_5 happens between 1 and 5 min of annealing, activating fast surface migration. The morphology of single-crystalline nanorods dominated by the low-energy (001) surfaces and with the [010] growh direction appears next. The nanorods enlarge via their coalescence.

Performance in lithium-ion batteries

The V_2O_5 nanorods were tested in both cathodes and anodes of lithium-ion batteries. The electrochemical performance of V_2O_5 nanorods in a cathode has been initially assessed in our previous publication [5], and we summarize it here briefly. The discharge curve of the first cycle has several plateaus and voltage drops corresponding to phase changes. It is believed that, in agreement with literature [1, 8], V_2O_5 transforms sequentially into several $Li_xV_2O_5$ phases depending on the amount of lithium insertion. $\alpha-(x<0.01)$, $\varepsilon-(0.35<\times<0.7)$, $\delta-(x=1)$, $\gamma-(1<\times<3)$ and $\omega-(x=3)$ phases can be observed when more and more lithium is intercalated into vanadium oxide. A single slope charge and discharge curves in the second and subsequent cycles (Fig. 6a in [5]) are characteristic for cycling of ω-$Li_xV_2O_5$ phase, which cycles in a single solid-solution phase. The nanorods maintained a stable capacity of around 260 mAh/g for 50 cycles without significant degradation.

Figure 4 shows the comparison of the cyclic behavior of V_2O_5 nanorods and the commercial V_2O_5 powder (Sigma Aldrich). As it is outlined above, the capacity of nanorods stays at the level of around 260 mAh/g, while an obvious decline in the capacity of V_2O_5 powder is observed after 30 cycles. Good capacity retention can be correlated with the crystal orientation and decreased thickness of nanorods, which possibly minimizes the irreversible disintegration of particles. A similar stable cyclic behavior of V_2O_5 nanorods with identical crystalline orientations in a cathode of lithium-ion batteries has been observed in an independent study [9].

The results of the electrochemical testing in an anode are shown in Fig. 5. The discharge curve in the first cycle (Fig. 5a) shows several plateaus at 3.1–3.3, 2.6–2.8, 2.3–2.4, 1.9–2.1, and 0.01–0.9 V, respectively. These plateaus are believed to correspond to phase transitions and are found to be similar to those reported for V_2O_5 previously [10]. The observed discharge capacity in the first cycle in the commercial and nanorod powders are about 1,060 and 1,398 mAh/g, respectively. The capacity of nanorods is close to the theoretical capacity of 1,471 mAh/g suggested by Liu et al. [4] on the basis of assumption of the full reduction of V from V^{5+} to metallic state. The first charge curve exhibits a less sloping voltage profile, with two inconspicuous plateaus and a lower capacity of 534 and 608 mAh/g, respectively. It can be calculated that the initial coulombic efficiency is 50.4% and 43.5%, respectively. The discharge capacity in the second cycle for the electrode made of V_2O_5 nanorods is 624 mAh/g and the capacity reaches the level of about 461 mAh/g after the 20th cycle. The discharge capacity for the electrode made of the reference V_2O_5 powder is 521 mAh/g in the second cycle and 394 after the 20th cycle. The capacity retention between the second and 20th cycles for the commercial powder and nanorods was calculated to be about 73 and 74%. Despite its lower initial columbic efficiency, V_2O_5 nanorods show slightly better capacity and capacity retention than those of commercial powder (Fig. 5b).

Based on the obtained electrochemical data, we can conclude that the nanorods provide a better cycling stability than that of the commercial powder in a cathode while the performance of two materials is comparable in an anode. The differences are likely to relate to different mechanisms of operation of V_2O_5 in cathodes and anodes of lithium-ion batteries.

As it is widely accepted now, V_2O_5 gets transformed into the ω-$Li_xV_2O_5$ phase in the cathode during the first

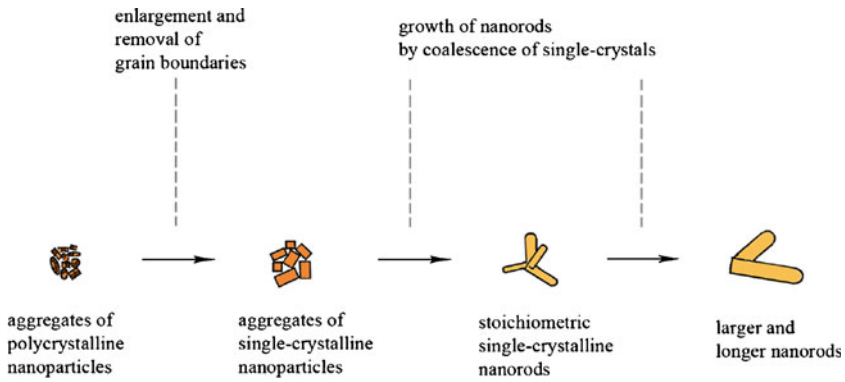

Fig. 3 The scheme illustrating the formation of V_2O_5 nanorods

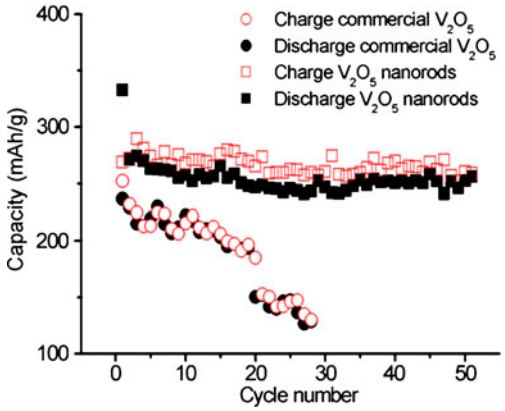

Fig. 4 The charge and discharge capacities of electrode based on V_2O_5 nanorods and on the reference powder as functions of cycle number. The cells were cycled between 1.5 and 3.5 V. The current rate was set at 10 mA/g

discharge, and further charging and discharging happens within this new phase [1, 8]. Chan et al. have studied lithiation/delithiation of V_2O_5 nanoribbons [11]. The single-crystalline nanoribbons had crystalline structures and orientations identical to those of our nanorods—a rectangular cross section, elongation along the [010] crystallographic direction and the suppressed thickness along the [001] direction. It has been observed that the V_2O_5 nanoribbons with the smallest thickness and width could transform reversibly into nanoribbons of ω-$Li_xV_2O_5$. Larger nanoribbons could be lithiated into nanoribbons of ω-$Li_xV_2O_5$, but the signs of stress and textured polycrystalline structure as well as domains of γ-$Li_xV_2O_5$ were detected by TEM. Large or randomly shaped particles of V_2O_5 have been considered to lose structural integrity upon lithiation. We can correlate our data to these observations. The nanorods are capable of operating reversibly after partial transformation into the ω-$Li_xV_2O_5$ phase, while particles with random crystalline orientation and sizes in the commercial V_2O_5 powder tend to get disintegrated gradually upon cycling.

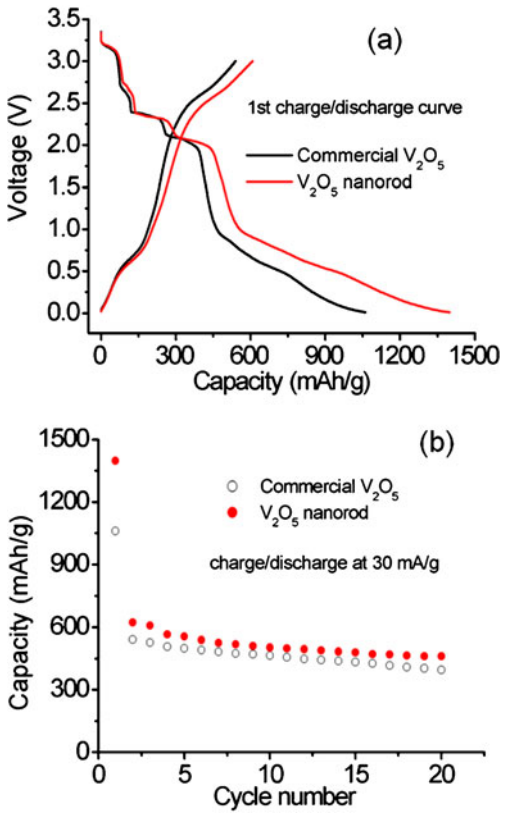

Fig. 5 **a** Charge–discharge curves for the first cycle and **b** discharge capacity vs. cycle number curves of the electrodes made from commercial V_2O_5 powder and as-synthesized V_2O_5 nanorod

Although the mechanism of the use of V_2O_5 in anodes is not clear, it can possibly be via a conversion reaction or via an alloying/dealloying process. A range of transition metal oxides have been reported to be active as anode materials for lithium-ion batteries, and most of these materials operate via the mechanism of the conversion reaction. The detailed studies show that the uptake of Li transforms transition metal oxides into an M/Li_2O nanocomposite in which the small metal grains are embedded in an amorphous Li_2O matrix [12, 13]. The process of Li uptake/extraction is reversible in a voltage range of 0–3 V with about 75% coulombic efficiency at the first cycle and nearly 100% coulombic efficiency in the following cycles. The range of materials that can be involved in the conversion reaction includes numerous transition metal oxides such as those of Fe, Ni, Co, and Cu [12]. Another possibility is an alloying/dealloying process similar to the case of SnO_2. This alloying/dealloying process was proposed by Anani et al. [14] in order to explain the large capacity fading when Sn metal was used as electrode. For a SnO_2 electrode, the process consists of a two-step reaction with lithium. The initial step involves the irreversible reduction of the tin oxide to tin metal particles in a lithium oxide matrix. The second step is the reversible alloying of the Li^+ with the tin metal [14].

At the same time, both reaction mechanisms outlined above have been denied as representative mechanisms for vanadates in anodes by Denis et al. [15]. These authors proposed that some lithium–oxygen interactions took place during the electrochemical reduction of vanadates, which resulted in the linkage of Li to oxygen. The formation of "Li–O" bonds was believed to be one of the reasons for the large polarization between charge and discharge. Denis et al. concluded that breaking the oxygen–Li bond required an energy larger (e.g., a larger electrochemical potential) than the energy necessary to remove an inserted Li-ion from an open-framework structure. Therefore, a possible scenario for the Li acceptance/removal into these vanadates is that, besides the reduction/oxidation of a vanadate, there are "Li–O" interactions on the noncoordinated oxygen atoms.

Some other reports such as those by Leroux et al. on molybdenum oxides ($Na_{0.25}MoO_3$) [16] and vanadates ($MnV_2O_{6.96}$) [17] used this idea to explain their data. Leroux and coworkers demonstrated the occurrence of a decomposition mechanism (leading to a "Li–O" matrix together with a $Li_xNa_{0.25}MoO_3$ and $Li_xMnV_2O_{6.96}$). In the same work, Leroux et al. have also pointed out the necessity of oxygen transport during the discharge/charge process. The work of Ceder at al. involving a series of computational experiments [18] on $LiMO_2$ (M=Ti, V, Mn, Co) gives another evidence to support the formation of Li–O bond. They have found that Li intercalation causes significant electron transfer to the oxygen ions in the structure. These results suggest that the uptake/removal mechanism in the V_2O_5 and related vanadate phases can be different from those of usual Li insertion/deinsertion, conversion reaction, or alloying/dealloying processes. In order to understand the electrochemical reaction mechanism, further experimental works, such as in situ synchrotron analysis are needed, and the future results will be published elsewhere.

Conclusions

Ball milling of V_2O_5 powder and the subsequent recrystallization in air represent a prospective method for growing V_2O_5 nanorods with attractive electrochemical properties. A fluidized bed is capable of minimizing sintering in the powder of nanorods. Additional experiments have shown that the initial stage of ball milling reduces the oxide to some extent and creates a nanocrystalline structure with the grain size in the range of 7–35 nm. The individual particles are becoming single-crystalline and the material oxidizes gradually during the annealing at around 600 °C. Stoichiometric nanorods are formed after 5 min of annealing. The growth of nanorods dominated with {001} facets is driven by the minimization of surface energy, and surface diffusion plays an important role in the growth process.

The nanorods have been tested as a cathode and anode material in lithium-ion batteries. The performance is directly compared with that of a commercially available V_2O_5 powder (Sigma Aldrich). The nanorods show a more stable cyclic behavior in a cathode, which can be attributed to the suppressed size and beneficial morphology. The morphology (shape and crystal orientation of nanorods) helps to avoid drastic disintegration when the material is transformed into the ω-$Li_xV_2O_5$ phase and cycled within this phase as a cathode material. As an anode material, V_2O_5 nanorods show a very high capacity of about 1,400 mAh/g in the first discharge, which drops significantly to 450–650 mAh/g in the second and following cycles. The performance of V_2O_5 as an anode material is less morphology sensitive and is somewhat similar for V_2O_5 nanorods and the reference powder.

Acknowledgements The work is supported in part by the Australian Research Council under the Centre of Excellence and Discovery programs. The authors thank the staff of the Electron Microscopy Unit at the Australian National University (Canberra, Australia) for their assistance with SEM and TEM analysis.

References

1. Wang Y, Cao GZ (2006) Chem Mater 18:2787–2804
2. Wang Y, Cao GZ (2008) Adv Mater 20:2251–2269
3. Tranchant A, Messina R, Perrichon J (1980) J Electroanal Chem 113:225–232
4. Liu J, Xia H, Xue DF, Liu L (2009) J Am Chem Soc 131:12086–12087
5. Glushenkov AM, Stukachev VI, Hassan MF, Kuvshinov GG, Liu HK, Chen Y (2008) Cryst Growth Des 8:3661–3665
6. Glushenkov AM, Stukachev VI, Hassan MF, Kuvshinov GG, Liu HK, Chen Y (2010) Proceedings of 2009 MRS Spring Meeting, in press
7. Occhiuzzi M, Cordischi D, Dragone R (2005) J Solid State Chem 178:1551–1558
8. Delmas C, Cognac-Auradou H, Cocciantelli JM, Menetrier M, Doumerc JP (1994) Solid State Ionics 69:257–264
9. Ban CN, Chernova NA, Whittingham MS (2009) Electrochem Commun 11:522–525
10. Poizot P, Laruelle S, Grugeon S, Dupont L, Tarascon JM (2000) Ionics 6:321–330
11. Chan CK, Peng H, Twesten RD, Jarausch K, Zhang XF, Cui Y (2007) Nano Lett 7:490–495
12. Poizot P, Laruelle S, Grugeon S, Dupont L, Tarascon JM (2000) Nature 407:496–499
13. Debart A, Dupont L, Poizot P, Leriche JB, Tarascon JM (2001) J Electrochem Soc 148:A1266–A1274
14. Anani A, Crouch-Baker S, Huggins RA (1987) J Electrochem Soc 134:3098–3102
15. Denis S, Baudrin E, Touboul M, Tarascon JM (1997) J Electrochem Soc 144:4099–4109
16. Leroux F, Gowards GR, Power WP, Nazar LF (1998) Electrochem Solid State Lett 1:255–258
17. Leroux F, Piffard Y, Ouvrard G, Mansot JL, Guyomard D (1999) Chem Mater 11:2948–2959
18. Ceder G, Aydinol MK, Kohan AF (1997) Comput Mater Sci 8:161–169